

Investigating thermo-physical properties and thermal performance of Al_2O_3 and CuO nanoparticles in Water and Ethylene Glycol based fluids

Bahman Rahmatinejad¹, Mahdi Abbasgholipour^{2,*}, Behzad Mohammadi Alasti²

¹Phd student, Department of Biosystem Mechanical engineering, Bonab Branch, Islamic Azad University, Bonab, Iran

²Assistant Professor, Department of Biosystem Mechanical engineering, Bonab Branch, Islamic Azad University, Bonab, Iran

Received 20 December 2020; revised 18 April 2021; accepted 29 April 2021; available online 04 May 2021

Abstract

The thermophysical properties and thermal performance of water- and ethylene-glycol-based nanofluids containing Al_2O_3 and CuO nanoparticles were examined. Nanofluids were prepared at four concentrations (1-4 vol%) using an electric mixer and magnetic stirrer, and the thermophysical properties were measured. Surfactants were used to improve stability. The transient hot-wire method (KD2-Pro device), Dynamic Light Scattering (DLS), and Ostwald viscometer (ASTM D445-06) were used to measure the resulting thermal conductivity coefficient, nanoparticle diameter, and nanofluid viscosity, respectively. The experiments were carried out in the 20 to 50 °C temperature range. Adding 1 wt% sodium dodecyl sulfate (SDS) to the CuO-water and the same amount of sodium dodecylbenzene sulfonate (SDBS) to the Al_2O_3 -water nanofluid were found to stabilize them for 20 and 22 days, respectively. Increasing the nanoparticle volume fraction, raising the temperature, and reducing nanoparticle diameter were found to increase the thermal conductivity coefficient. The density also increases with the nanoparticle volume fraction in the base fluid increasing. Moreover, at the same volume fraction, the CuO-water nanofluid had a higher density than Al_2O_3 -water. Better base fluid thermal properties amplify the effect on the nanofluid's thermal conductivity coefficient. The actual thermal conductivity coefficient was determined by comparing model predictions of the coefficient.

Keywords: Al_2O_3 ; CuO; Nanofluids; Nanoparticles; Thermal Conductivity Coefficient.

How to cite this article

Rahmatinejad B., Abbasgholipour M., Mohammadi Alasti B Investigating thermo-physical properties and thermal performance of Al_2O_3 and CuO nanoparticles in Water and Ethylene Glycol based fluids. *Int. J. Nano Dimens.*, 2021; 12(3): 252-271.

INTRODUCTION

Heat transfer is one of the most important processes in many industrial and consumer products. For more than a century, scientists and engineers have made great efforts to enhance the inherently poor thermal conductivity of conventional fluids. So the idea of dispersing solid particles in fluids, which started with millimeters and micrometers, was completed with the use of solid nanoparticles, and today nano-fluids are a good alternative to normal fluids such as water and

oil [1]. Nano particles cause a significant increase in the heat transfer of nano-fluids. Adding nano particles to the base liquid has a significant effect on thermal conductivity. Many researchers have extensively investigated nanofluids in terms of their thermal and dynamic properties, the ability to develop these properties, and the possibilities of using them in industrial applications [2-3]. In 1995, for the first time in the laboratory, a scientist called Choi significantly increased the production and thermal conductivity coefficient of a base fluid in a combination of solid metal and non-metallic nanoparticles in conventional fluids. He called the

* Corresponding Author Email:

abbasgholipour@bonabiau.ac.ir

resulting suspension nanofluid [4]. After Choi, most researchers focused on increasing the thermal properties of nanofluids. A number of these studies are listed below. Morshed *et al.* examined the nanoparticles of copper dioxide in water in the range of 0.5 to 5%. They observed the nonlinear behavior of the conductivity coefficient with volume deduction, especially in low volume deductions. [5]. Das *et al.* studied the nanofluid behavior of water and copper oxide, as well as water and aluminum oxide, by changing the temperature. They concluded that as the temperature increases, the thermal conductivity of the nanofluid increases [6]. Karthik *et al.* investigated the thermal conductivity coefficient of copper oxide nanofluid. Their studies have shown that temperature has significant effects on the thermal conductivity coefficients of nanofluids [7]. Kucharska *et al.* examined the effect of adding a coating AL_2O_3 cover on nickel. The results showed that the obtained piece has more stiffness and abrasion resistance than pure nickel [8]. Ghazvini *et al.* in their experimental study, investigated the effect of copper oxide nanoparticle concentration on increasing viscosity and thermal conductivity coefficient of SAE 20W50 engine oil at concentrations of 0.1% to 0.5% and for temperatures of 40 to 100°C [9]. Leong *et al.* examined the effect of using ethylene glycol-copper nanofluid as a coolant in a car's radiator. The results showed that adding 2% of nanoparticles to the base fluid increased the thermal conductivity coefficient rate by 4% [10]. Leong *et al.* investigated the effect of changes in the thermal conductivity coefficient of nanofluid copper-ethylene glycol on car radiators. The results showed that increasing the Reynolds number of air and cooling fluid increased the thermal conductivity coefficient [11]. Syam Sundar *et al.* showed that the viscosity of nanofluids depends on the concentration of particles, temperature, size, and shape of the particles and the viscosity of the base fluid. In addition to the above, how to stabilize nanofluids, how to make and synthesize nanoparticles and the nanoparticle manufacturer are effective in the viscosity of nanofluids [12]. Pugalenthil *et al.* studied the reinforcing effect of Sic and AL_2O_3 on aluminum composite. They produced four samples by casting method and showed that the reinforcement material increases the tensile strength, resistance, and hardness of the matrix aluminum [13]. Pastoriza-Gallego *et al.* investigated the effect of particle size on viscosity

and volumetric behavior of CuO nanofluid. The results showed that the effect of particle size on density is low but not negligible, but this effect on viscosity is very large and should be considered in any scientific application [14]. Singh *et al.* measured the changes in the rate and thermal conductivity coefficient vertically and horizontally by changing the difference between the temperature of the steam and the surface on the thermal pipes. The findings show that the thermal conductivity coefficient rate using copper nanofluid for vertical pipe mode is 2.07 times higher than the horizontal pipe mode and the thermal conductivity coefficient in the vertical mode is 1.94 times higher than the horizontal mode [15]. Turkyilmazoglu used the classic Nusselt layer-density theory and presented two different analytical models for nanofluids. In this analysis, he used silver nanoparticles, copper, copper oxide, aluminum oxide, and titanium oxide with a water-based fluid. His results show that by increasing the volume deduction of nanoparticles, the thickness of the condensed layer decreases and it increases the thermal conductivity coefficient, too [16]. El Mghari *et al.* numerically analyzed the thermal conductivity coefficient at the nano scale layer density within the square micro channel. Their results show that if the volume deduction of copper nanoparticles increases by 5%, the thermal conductivity coefficient improves by 20% [17]. Azimi and Taheri showed in their study that, an empirical electrical conductivity assessment of nanofluids comprising CuO nanoparticles water-based in different concentrations, particles size and various temperatures of nanofluids has been carried out in this paper. These experimentations have been done in deionized water with nanoparticles sizes such as 89, 95, 100 and 112 nm and concentrations of 0.12 g/l, 0.14 g/l, 0.16 g/l and 0.18 g/l so nanofluids obtain in temperatures such as 25 °C, 35 °C, 45 °C and 50 °C for investigation of their electrical conductivity. It is observed that, in water-based nanofluids, the electrical conductivity increases with increasing in both nanofluids temperatures and concentration respectively in the range 25–50°C and 0.12-0.18g/l. But in nanoparticles size rising in nanofluids we observe that electrical conductivity has a few increases when nanoparticles have 95nm diameters, so decrease for biggest nanoparticles such as 100 and 112nm. It seems that there is an optimum in electrical conductivity with various nanoparticles. [18]. Sabbaghi *et al.* by use of nonionic surfactants polyethylene glycol (PEG),

the clew CuO nanostructure with the diameter of about 4 μm was prepared at 150 $^{\circ}\text{C}$ for 11 hr. As the temperature increased to 160 $^{\circ}\text{C}$ for 11 hr, the gear wheel CuO nanostructure with the diameter of about 70 nm was made. Furthermore, two other temperatures (180 and 200) are utilized for 20 hr to produce nanowire. The product was characterized by powder X-Ray diffraction, and scanning electron microscopy SEM showed the various shapes of CuO nanostructures, including clew, gearwheel, and nanowire bundles. [19]. Bhuiyan *et al.* conducted a study on the surface tension of alumina nanoparticles and titanium dioxide. It was determined that the surface tension of the fluid and the angle of contact of the droplet with the surface is one of the influential parameters in droplet density [20]. The use of nanofluid as a fluid with advanced thermal conductivity coefficient properties in various industries is increasing. Therefore, determining the thermo-physical properties of these fluids is important. Due to the lack of similar studies in this regard, and the inefficiency of classical relationships in determining the exact coefficient of thermal conductivity coefficient of nanofluids on the one hand and on the other hand providing contradictory results by researchers in this regard led us to do the present research. Therefore, these properties were determined in a laboratory and compared with valid sources in order to evaluate the accuracy of the obtained cases. Nanofluids were used in heat exchangers, oscillating heat pipes, chillers, solar water heating machining, car engine cooling, electronic component cooling, and nuclear reactor cooling.

MATERIALS AND METHODS

This section, first, discusses base fluid preparation, which could be water or Ethylene Glycol (EG), before reviewing the production of nanoparticles with a Plasma Nano Colloid Maker (PNC1k-C) and their electron microscope imaging. Next, nanoparticle diameter measurement by Dynamic Light Scattering (DLS) and, finally, the evaluation of the thermophysical parameters in different conditions using a KD2 Pro thermal properties analyzer are described.

Distilled Water Preparation

Distilled water is required to produce a water-based nanofluid. In this study, the required distilled water was produced using a Fater Electronics

Model 6004 device.

Nanoparticle Production

The PNC1k-C produces metal nanocolloids on a laboratory scale by the electrical wire explosion technique. Here, Al_2O_3 and CuO nanoparticles were prepared by this device.

Imaging of Nanoparticles

The Transmission Electron Microscope (TEM) is a specialized tool for revealing the materials' microstructure and morphology and enables microstructural studies of materials with extreme magnification at high resolution. Images were taken on an H9500 TEM and a HITACHI Su3500 scanning electron microscope (SEM). Figs. 1a and c show TEM images of Al_2O_3 and CuO nanoparticles. Moreover, Figs. 1b and d show SEM images of the two nanoparticles.

Nanoparticle Diameter Measurement by DLS

Light scattering methods are commonly used to determine particle size and size distribution in colloidal systems. In this method, a laser beam illuminates the suspension, recording the scattering patterns by an optical detector. Larger particles have a lower velocity in the solution than smaller ones. Therefore, the scattering pattern changes more slowly in a suspension with larger particles than one contain smaller particles.

The relationship between particle size and Brownian motion speed is established by the Stokes–Einstein relation: (Eq. 1).

$$d_H = \frac{KT}{3\pi\eta D} \quad (1)$$

d_H : Hydrodynamic Diameter of Particle, K : Boltzmann constant, η : solvent viscosity that depends on temperature and is not related to system density and pressure. T : Absolute temperature and D : Influence coefficient [20]. Fig. 2 shows the measurement of particle diameter histograms.

Nanofluid Preparation

Dry, analytical-grade pure Al_2O_3 and CuO nanoparticles with 10 nm and 50 nm particle sizes, products of Tamad Kala Co., were used. An electric agitator with adjustable speed (200–3000 rpm) was used to mix the nanofluid. Next, the

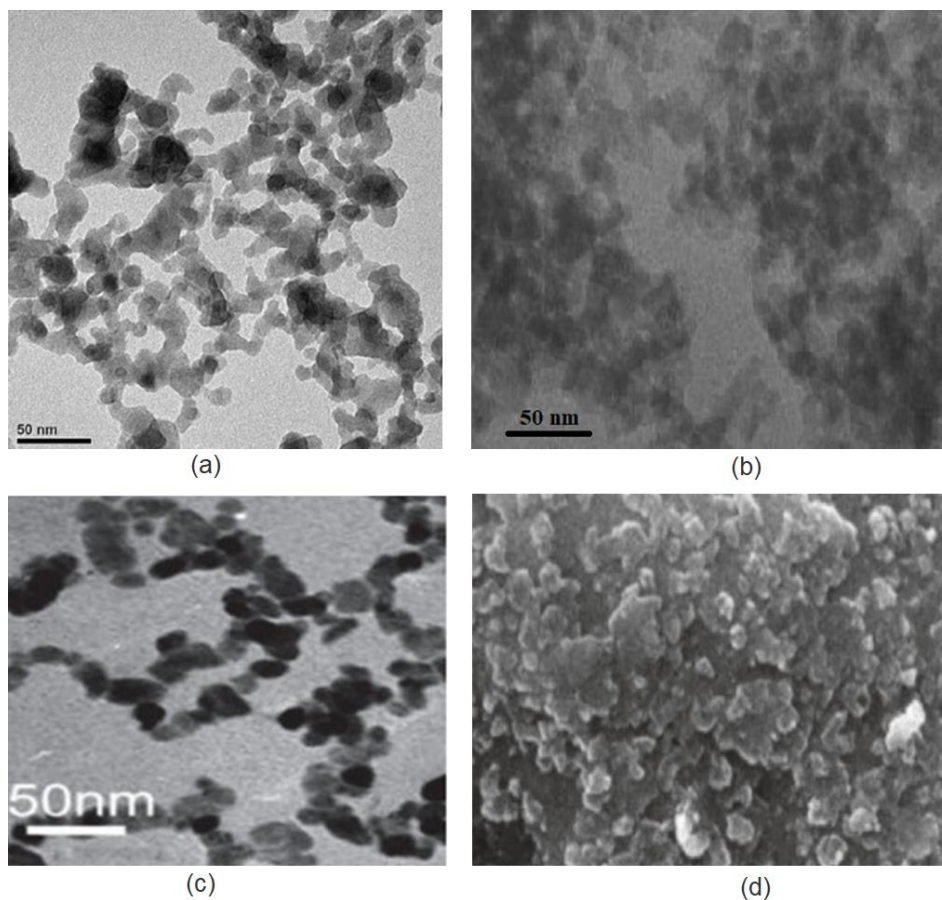


Fig. 1. (a) TEM image of Al₂O₃ nanoparticles, (b) SEM image of Al₂O₃ nanoparticles, (c) TEM image of CuO nanoparticles, (d) SEM image of CuO nanoparticles.

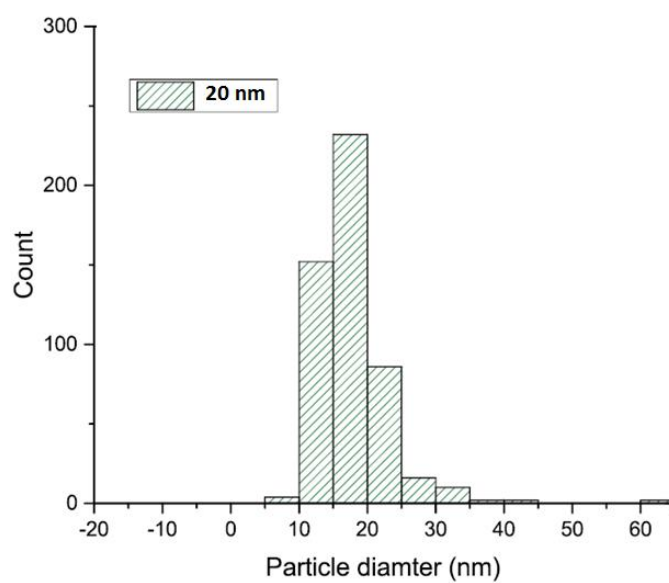
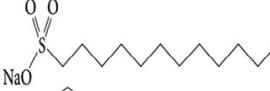
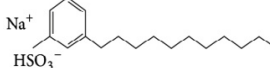


Fig. 2. Histogram for measuring the diameter of nanoparticles Al₂O₃.

Table 1. Specifications of surfactants.

surfactant	Molecular formula	Formula structure	Molecular Weight (g/mol)	Density ($\frac{g}{cm^3}$)
Sodium dodecyl sulfate [21]	$NaC_{12}H_{25}SO_4$		288.372	1.01
Sodium dodecyl benzene sulfonate [22]	$C_{18}H_{29}NaO_3S$		348.48	1.02

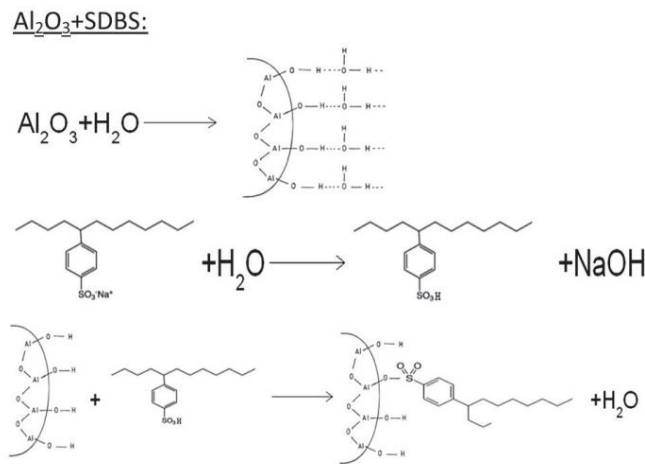


Fig. 3. Reaction mechanism between Al₂O₃ nanoparticles and sodium dodecyl benzene sulfonate.

solution was placed on a magnetic shaker with a speed range of 100–2000 rpm and 400 W heating powers. Equation 2 estimates the mass fraction (wt%) considering the mass of nanoparticles (m_p) and the mass of the base fluid (m_f) [65].

$$\phi = \left(\frac{m_p}{m_p + m_f} \right) \times 100 \quad (2)$$

Let ρ_p denote the nanoparticles' density and ρ_f the base fluid density. The volume fraction of nanoparticles (Φ) can be estimated from Eq. 3 [10].

$$\Phi = \frac{\frac{m_p}{\rho_p}}{\frac{m_p}{\rho_p} + \frac{m_f}{\rho_f}} \quad (3)$$

Surfactants were used to maintain the solution stability for engineering applications. The material

specifications are presented in Table 1.

As evident, 1 wt% sodium dodecyl sulfate (SDS) was added to the CuO nanofluid, and 1 wt% sodium dodecyl benzene sulfonate (SDBS) was used for the Al₂O₃ solution. These solutions were products of Kalazist Co. Fig. 3 illustrate the reaction between Al₂O₃ nanoparticles and sodium dodecylbenzene sulfonate.

Measuring the Nanofluid Thermal Conductivity Estimation Methods for the Thermal Conductivity Coefficient

Several experimental theories have been proposed for measuring thermal conductivity by theoretical methods, some of which have been employed in this study (Table 2).

Measuring Thermal Conductivity by the Transient Hot Wire Method

The Transient Hot Wire (THW) method is a common technique for the experimental measurement of the thermal conductivity of liquids by statistical means and using a linear

Table 2. Mathematical models for estimating thermal conductivity coefficient.

Explanations	Mathematical model	Model
Most primitive model by assuming particles in spherical shape.	$K_{eff} = \frac{K_p \phi_p (dT/dx)_p + K_b \phi_b (dT/dx)_b}{\phi_p (dT/dx)_p + \phi_b (dT/dx)_b}$	Maxwell [23]
The modified model is Maxwell and it is in good agreement with the experimental data.	$\frac{K_{nf}}{K_f} = \frac{(K_p + 2K_f) - 2\phi(K_f - K_p)}{(K_p + 2K_f) + \phi(K_f - K_p)}$	Maxwell-Garnett [24]
Applicable to spherical particles (n = 3) and cylindrical particles (n = 6)	$K_{eff} = \frac{K_p + (n - 1)K_1 - (n - 1)(K_1 - K_p)\phi}{K_p + (n - 1)K_1 + (K_1 - K_p)\phi} K_1$	Hamilton [25]
Assuming spherical and binary interaction between particles.	$K_{eff} = [1 + 3\beta\phi + (3\beta^2 + \frac{3\beta^3}{4} + \frac{9\beta^3}{16} - \frac{\alpha + 2}{2\alpha + 3} + \frac{3\beta^4}{2^6} + \dots)\phi^2]k_1$	Jeffrey [26]
Assuming spherical and non-spherical particles.	$K_{eff} = [1 + a\phi + b\phi^2]k_1$ a = 2.25, b = 2.27 for $\alpha = 10$; a = 300, b = 4.51 for $\alpha = \infty$	Loo – Lin [27]
In this model, the only effective parameter is the volume percentage.	$\frac{K_{nf}}{K_f} = (1 + 3\phi)$	Timofeeva [28]
In this model, the only effective parameter is the volume percentage.	$\frac{K_{nf}}{K_f} = 1 + 7.47\phi$	Pak – Cho [29]

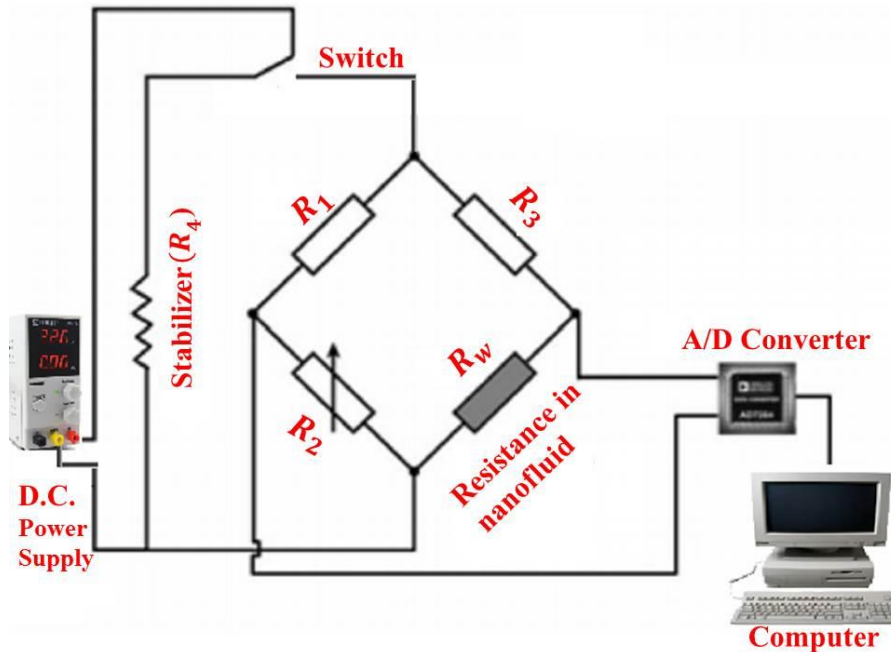


Fig. 4. Measurement of thermal conductivity coefficient using transient hot wire.

source. A thin metal wire made of platinum (or tantalum) measuring 5-80 μm in diameter is placed inside the liquid, serving as both a heat source and a thermometer. The specimen's thermal conductivity can be determined from the temperature variation of the hot wire over time. The wire's thermal resistance changes with temperature. A Wheatstone bridge measures the electrical resistance of the R_w wire. The electrical

resistance of the R_3 potentiometer is set when the galvanometer G shows zero current. By balancing the bridge with the zero galvanometer current, the value of R_w (Eq. 4) can be determined based on the known values of R_1 , R_2 , and R_3 (Fig. 4)

$$R_w = \frac{R_1 R_2}{R_3} \tag{4}$$

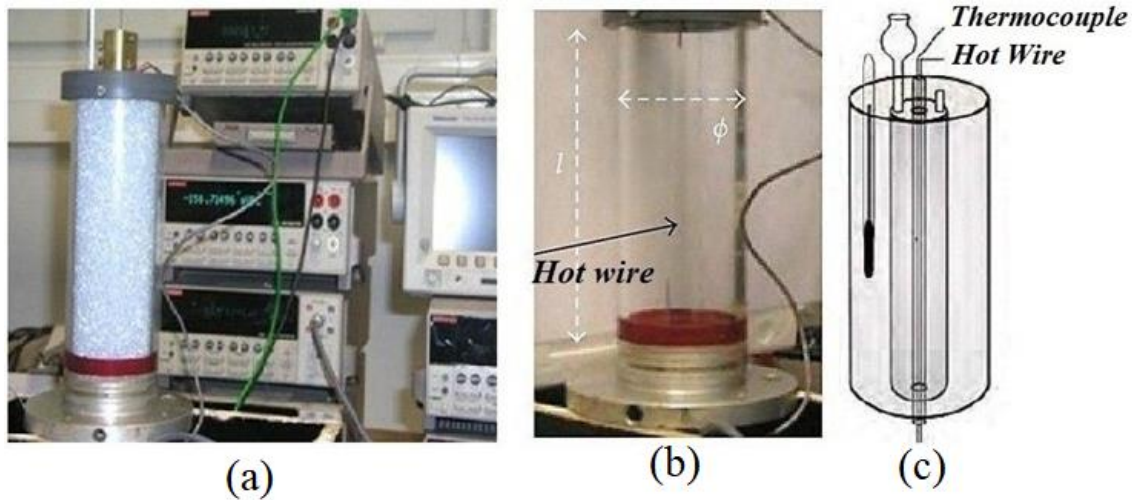


Fig. 5. View of the Hot Wire device for measuring thermal conductivity, (a) Main device, (b) Hot wire housing, (c) Thermocouple.

Since nanofluids are electrical conductors, covering the platinum wire with a thin layer of electrical insulator will prevent such problems as the electric current running through the fluid causing heat generation in the wire. This technique, referred to as the modified THW, was introduced by Nagasaka and Nagashima, who covered the wire in a layer of epoxy adhesive [31]. Given the platinum wire's small diameter and high electrical conductivity, it can be assumed as a linear source in an unlimited cylindrical environment. This study uses the relationships proposed in the literature for this setting (Eqs. 5–9) [34]. Transient temperature for a long time follows the following relationship.

$$T(r,t) = \frac{Q}{4\pi k} \left[\ln\left(\frac{4\alpha t}{r^2}\right) + \frac{r^2}{4\alpha t} - \frac{1}{4} \left(\frac{r^2}{4\alpha t}\right) - \dots - \gamma \right] \quad (5)$$

In this equation:

Q: The applied power per unit length in the heat source $\left(\frac{W}{m}\right)$

k: Thermal conductivity coefficient $\left(\frac{W}{m.K}\right)$

α : Thermal distribution coefficient $\left(\frac{m^2}{s}\right)$

r: radial position of temperature measurement

Y: The stability of Uller is $\gamma = \ln(\sigma) = 0.57721$

This approximation can be used for a linear source located within an unlimited cylindrical environment: [32].

$$\left(\frac{r^2}{4\alpha t}\right) \ll 1 \quad (6)$$

Therefore, the equation becomes as follows [32].

$$T(r,t) = \frac{Q}{4\pi k} \left[\ln\left(\frac{4\alpha t}{r^2}\right) - \gamma \right] = \frac{Q}{4\pi k} \left[\ln t + \ln\left(\frac{4\alpha}{r^2}\right) - \gamma \right] \quad (7)$$

Therefore, the dependence of temperature on time is as follows, which we will have in two different times: [32].

$$\Delta T = T(t_2) - T(t_1) = \frac{Q}{4\pi k} \ln\left(\frac{t_2}{t_1}\right) \quad (8)$$

By placing Q and simplifying the following equation for k is obtained [32].

$$k = \frac{Q}{4\pi [T(t_2) - T(t_1)]} \ln\left(\frac{t_2}{t_1}\right) \quad (9)$$

The transient hot wire method allows us to measure k quickly and accurately, while also reducing the unwanted effects of thermal conductivity (Fig. 5a, 5b, 5c).

Measuring Thermal Conductivity Using the KD2-Pro

The thermal conductivity of the nanofluids was measured using the KD2-Pro, a hand-held device for measuring thermal properties with manual controllers and sensors that can determine the thermal conductivity of nanofluids. The device comes with three accuracy settings (5-10%). The KS-1 sensor with a $\pm 5\%$ accuracy was used in the present study. The error can be reduced

Table 3. Thermo-physical properties of base fluids and nanoparticles [32].

Properties	Al ₂ O ₃	CuO	Copper	Ethylene glycol	Water
c_p (J kg ⁻¹ K ⁻¹)	765	533	385	2420.6	4179
ρ (kg m ⁻³)	3970	6500	8933	1110.2	997.1
K (W m ⁻¹ K ⁻¹)	40	76	400	0.253	0.613
$\beta \times 10^{-5}$ (K ⁻¹)	0.85	-----	1.67	57	21

by placing the specimen in a water bath with a 1 °C temperature difference from the sample. During data sampling, the specimen must remain stationary with the sensor installed perfectly perpendicular to the sample.

Table 3 lists the thermophysical properties of the base fluid and nanoparticles.

Determining the Density

The nanofluid density can be calculated using the law of mixtures and the Pak and Cho relation (Eq. 10) [34].

$$\rho_{\text{eff}} = \left(\frac{m}{V}\right)_{\text{eff}} = \frac{m_b + m_p}{V_b + V_p} = \frac{\rho_b V_b + \rho_p V_p}{V_b + V_p} = (1 - \phi_p)\rho_b + \phi_p \rho_p \quad (10)$$

Where ϕ denotes the nanoparticle volume fraction, ρ is the density and index; p indicates the nanoparticles and b the base fluid. The DA130N digital portable density meter, produced by KEM, Japan, was used to measure the density.

Measuring the Viscosity

Viscosity is the measure of a fluid's resistance to deformation under applied longitudinal or shear stress. Studies have shown that nanofluids have a higher viscosity than base fluid. Viscosity, similarly to conductivity, depends on the nanoparticle volume fraction. As illustrated by Table 4, various theoretical models have been proposed for calculating the viscosity of nanofluids. The ASTM D445-06 Ostwald Viscometer was used for measuring the viscosity here.

RESULTS AND DISCUSSION

CuO and Al₂O₃ Sedimentation in the Water-Based Nanofluid

Suspension uniformity and stability considerably improve the nanofluids thermal properties. Cluster formation or particle accumulation is a phenomenon that affects nanofluid stability and promotes particle settlement. Clustering has two adverse effects on the nanofluid. It could destabilize the suspension by creating large masses and also compromise

thermal conductivity by creating areas depleted of nanoparticles in the liquid, thus increasing the thermal resistance. This issue is illustrated in Fig. 6.

According to Fig. 6, nanoparticle aggregation and clustering becomes more likely as the volume fraction of nanoparticles scattered in the base fluid increases, reducing the thermal conductivity. A 1 vol% nanofluid was prepared with 20 nm nanoparticles to measure the settling time. An electric mixer was used in the first experiment to make a perfectly homogeneous solution. Then, 100 ml of the mixture was poured into a graduated container and photographed at regular intervals. Results showed that the mixture maintains its suspension state in the first hour, with some of the nanoparticles settling during the next hour. In the second experiment, the mixture was placed on a magnetic stirrer for 10 minutes, with the temperature set at 30 °C to delay nanoparticle settlement. The second solution was also photographed at regular intervals for comparison. In this experiment, the solution remained in a suspension state for 2 to 2.5 hours before it started to precipitate gradually. However, no surfactant was used to stabilize the solution. It was found that using an electric mixer (Figs. 7a and 8a) followed by magnetic stirring (Figs. 7b and 8b) to agitate the nanofluid produces a more stable nanofluid (Figs. 7c and 8c). The results are in agreement with previous reports [33]. The solution stability was further improved by adding 1 wt% SDS to the CuO nanofluid and 1 wt% SDBS to the Al₂O₃ nanofluid, helping them maintain stability for 22 (Fig. 7d) and 20 days (Fig. 8d), respectively.

The Actual and Theoretical Thermal Conductivity Coefficients

Experimental data are suggestive of improvements in thermal conductivity at increased nanoparticle volume fractions. Al₂O₃ and CuO nanofluids with different concentrations (1, 2, 3, and 4 vol%) were tested, recalculated, and evaluated based on seven theories (Table. 5).

Table 4. Summary of nanofluids' viscosity models.

Row	Model name	Models	Remarks
1	Einstein [34]	$\frac{\mu_{nf}}{\mu_f} = 1 + 2.5\phi$	Spherical particles of very low volume fraction ($\phi < 0.02$)
2	Krieger and Dougherty [35]	$\frac{\mu_{nf}}{\mu_f} = \left[1 - \frac{\phi}{\phi_m}\right]^{-\eta\phi_m}$	Randomly mono dispersed and hard spheres with variable packing fraction
3	Neilson [36]	$\frac{\mu_{nf}}{\mu_f} = (1 + 1.5\phi)e^{\frac{\phi}{1-\phi_m}}$	Power law model valid for particle volume fraction more than 0.02
4	Mooney [37]	$\frac{\mu_{nf}}{\mu_f} = e^{\frac{k\phi}{1-k\phi}}$	Appropriate for self-crowding factor ($1.35 < k < 1.91$) and fitting parameter of 2.5
5	Batchelor [38]	$\frac{\mu_{nf}}{\mu_f} = (1 + 2.5\phi + 6.5\phi^2)$	Extension of Einstein model considering Brownian motion
6	Lundgren [39]	$\frac{\mu_{nf}}{\mu_f} = \left[1 + 2.5\phi + \frac{25}{4}\phi^2 + f(\phi^3)\right]$	Reduction of Einstein model formulated from Taylor series expansion of ϕ
7	Brinkman [40]	$\frac{\mu_{nf}}{\mu_f} = (1 - \phi)^{2.5}$	Formulated from Einstein model. Valid for continuous medium of particle concentrations less than 4 %
8	Chen et al. [41]	$\frac{\mu_{nf}}{\mu_f} = \left(1 - \frac{\phi_a}{\phi_m}\right)^{-2.5\phi_m}$ $\phi_a = \phi \left(\frac{a}{a}\right)^{3-D}$	Modified Krieger–Dougherty equation. Consider particle aggregates
9	Franken and Acrivos [42]	$\frac{\mu_{nf}}{\mu_f} = \frac{9}{8} \left[\frac{\left(\frac{\phi}{\phi_m}\right)^{\frac{1}{3}}}{\left(\frac{\phi_m - \phi}{\phi_m}\right)^{\frac{1}{3}}} \right]$	Valid for spherical particles and for $0.5236 \leq \phi \leq 0.7405$ ϕ_m is determined experimentally
10	Ward [43]	$\frac{\mu_{nf}}{\mu_f} = [1 + \eta(\phi_{eff} + 2.5\eta + (2.5\eta)^2 + \dots)]$	Exponential model for up to 35 % of spherical particles
11	Kitano [44]	$\frac{\mu_{nf}}{\mu_f} = \frac{1}{\left[1 - \left(\frac{\phi}{\phi_m}\right)^2\right]}$	Based on maximum particle volume fraction
12	Bicerano [45]	$\mu_{nf} = (1 + \eta\phi + K_H\phi^2)$	Considers volumetric effect on viscosity
13	Tseng and Chen [46]	$\frac{\mu_{nf}}{\mu_f} = 0.4513e^{0.6965\phi}$	Considers volume concentration for nickel/terpineol nanofluids
14	Graham [47]	$\frac{\mu_{nf}}{\mu_f} = \left(1 + 2.5\phi + 4.5 \left[\frac{1}{\left(\frac{h}{d_p} \left(2 + \frac{h}{d_p}\right)\right) \left(1 + \frac{h}{d_p}\right)^2} \right]\right)$	Modified form of Franken–Acrivos model. Considers particle radius and inter-particle spacing
15	Masoumi et al. [48]	$\mu_{nf} = \mu_f \left(1 + \frac{\rho_N V_b d_N^2}{72C\delta\mu_f}\right)$	Based on Brownian motion of particles and valid for alumina/water nanofluids
16	Pak and Cho [49]	$\frac{\mu_{nf}}{\mu_f} = (1 + 39.11\phi + 533.9\phi^2)$	Developed by taking room temperature as reference
17	Kulkarni [50]	$\ln(\mu_{nf}) = -\frac{(2.8751 + 53.548\phi - 107.12\phi^2)}{(1078.3 + 15857\phi + 20587\phi^2)} + \frac{1}{T}$	Valid for CuO–water nanofluids within a temperature range of 5–50 °C
18	Nguyen et al. [51]	$\frac{\mu_{nf}}{\mu_f} = (2.1275 - 0.0215T + 0.00027T^2)$	Temperature-dependent viscosity with particle volume fraction 1–4 %
19	Namburu et al. [52]	$\log(\mu_{nf}) = Ae^{-BT}$	Temperature-dependent model and valid for Al ₂ O ₃ nanofluids with 1–10 % volume fraction and –35 to 50 °C
20	Chandrasekhar et al. [53]	$\frac{\mu_{nf}}{\mu_f} = 1 + b \left(\frac{\phi}{1 - \phi_m}\right)^n$	Considers electromagnetic, mechanical and geometrical aspects
21	Abu-Nada [54]	$\mu_{nf} = -0.155 - \frac{19.582}{T} + 0.794\phi + \frac{2094.47}{T^2} - 0.192\phi^2 - 8.11 \frac{\phi}{T} - \frac{27463.863}{T^3} + 0.127\phi^3 + 1.6044 \frac{\phi^2}{T} + 2.1754 \frac{\phi}{T^2}$	Temperature-dependent model, valid for Al ₂ O ₃ nanofluids

Continued Table 4. Summary of nanofluids' viscosity models.

Row	Model name	Models	Remarks
22	Masud Hosseini [55]	$\frac{\mu_{nf}}{\mu_f} = \exp \left[m + \alpha \left(\frac{T}{T_0} \right) + \beta(\phi_h) + \gamma \left(\frac{d}{1-r} \right) \right]$	Temperature-dependent model. Considers hydrodynamic volume fraction and thickness of capping layer
23	Avsec and Oblac [56]	$\frac{\mu_{nf}}{\mu_f} = [1 + 2.5(\phi_{eff} + 2.5\phi_{eff} + (2.5\phi_{eff}^2) + \dots)]$	Extension of Ward model and Einstein model

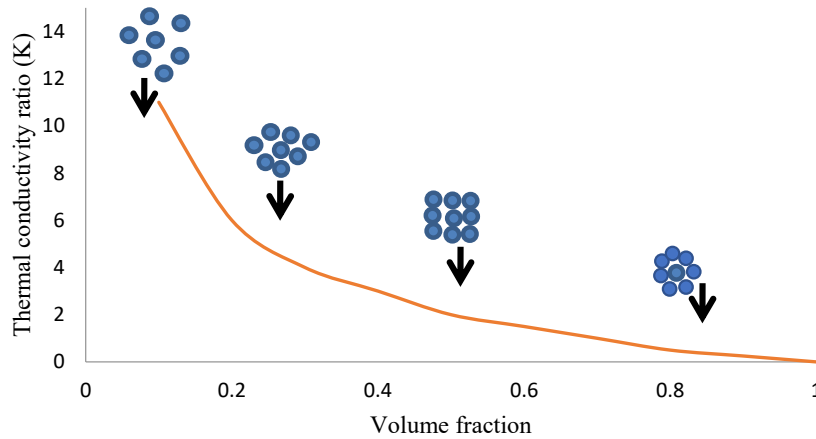


Fig. 6. Clustering effect and volume percentage on thermal conductivity coefficient [57].

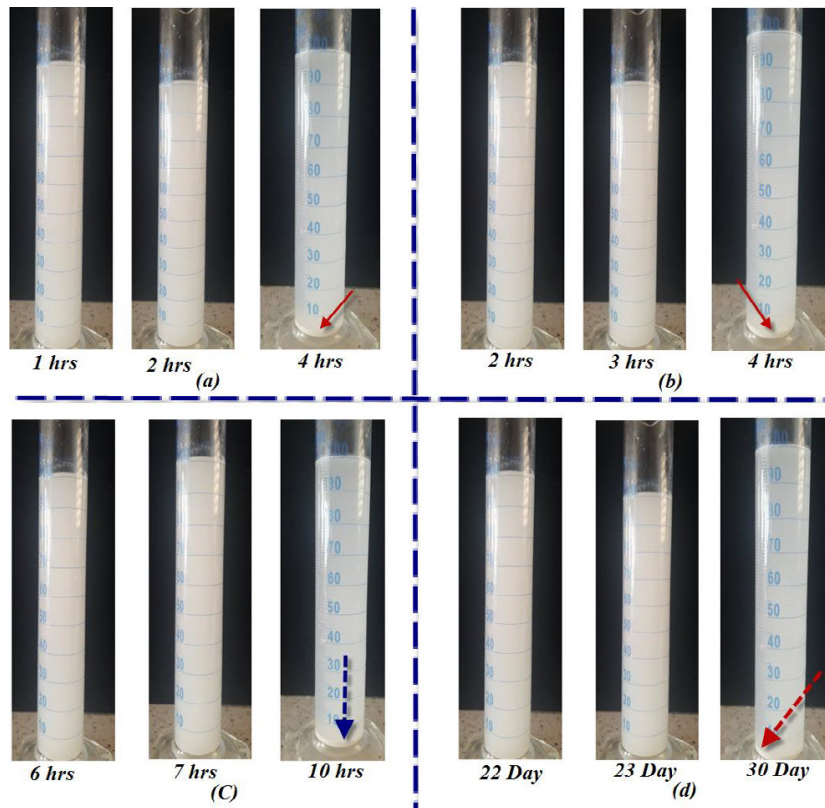


Fig. 7. Al₂O₃ Nano-fluid stability test (a) Using a conventional mixer (b) Using a magnetic stirring (c) Using an electric mixer and a magnetic stirring (d) Using an electric mixer and a magnetic stirring with surfactant.

Table 5. Determination of thermal conductivity coefficient by changing the volume deduction for nanofluid copper oxide in water.

	Jeffrey	Hamilton	Maxwell-Garnett	Maxwell	Timofeeva	Pak-Cho	Loo-Lin	experimental
Volume fraction (%)	K_{nf}/K_f	K_{nf}/K_f	K_{nf}/K_f	K_{nf}/K_f	K_{nf}/K_f	K_{nf}/K_f	K_{nf}/K_f	K_{nf}/K_f
1	1.029	1.057	1.03	1.029	1.03	1.074	1.022	1.039
2	1.06	1.116	1.061	1.59	1.06	1.149	1.045	1.068
3	1.091	1.176	1.092	1.09	1.09	1.224	1.069	1.091
4	1.123	1.238	1.124	1.121	1.12	1.298	1.093	1.132

$$K_f = 0.067, \alpha = 1141.79, \beta = 0.9973, n = 3, K_p = 76.5$$

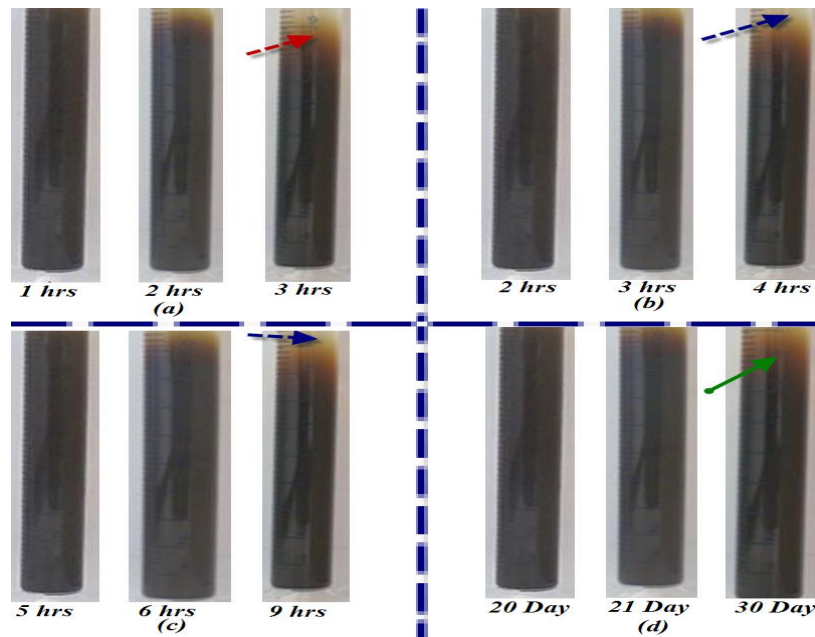


Fig. 8. CuO Nano-fluid stability test (a) Using a conventional mixer (b) Using a magnetic stirring (c) Using an electric mixer and a magnetic stirring (d) Using an electric mixer and a magnetic stirring with surfactant.

Experimental data and theoretical results determine the thermal conductivity coefficient, indicating an increase in thermal conductivity coefficient at higher volume fractions. In this analysis, Loo-Lin's theory predicts the lowest, and Pak-Cho's theory the highest thermal conductivity. Based on the regression of the calculated experimental results ($R = 0.99$), this value corresponds to the Timofeeva model (Fig. 9).

Effect of Nanoparticle Diameter on the Nanofluid's Thermal Conductivity

The thermal conductivity coefficients of CuO-water nanofluids with different concentrations (1–4 vol%) of 10 and 25 nm nanoparticles were examined, and Fig. 10 presents the results.

The thermal conductivity coefficients of Al_2O_3 -

water nanofluids with different concentrations (1 to 4 vol%) of 6, 10, and 20 nm nanoparticles were also examined, depicting the results in Fig. 10.

It was found that smaller suspended nanoparticles increase the thermal conductivity to a greater extent thanks to the higher surface-area-to-volume ratio. Reducing the size of the nanoparticles increases the surface area that is in contact with the fluid. Moreover, a comparison between CuO and Al_2O_3 nanofluids with 10 nm nanoparticles at the same volume fraction shows the higher thermal conductivity of CuO-water. This outcome can be attributed to the higher thermal conductivity of CuO nanoparticles. Further, reducing the particle diameter in the 4 vol% Al_2O_3 nanofluid from 20 to 10 nm increased the thermal conductivity by 9%. In the case of



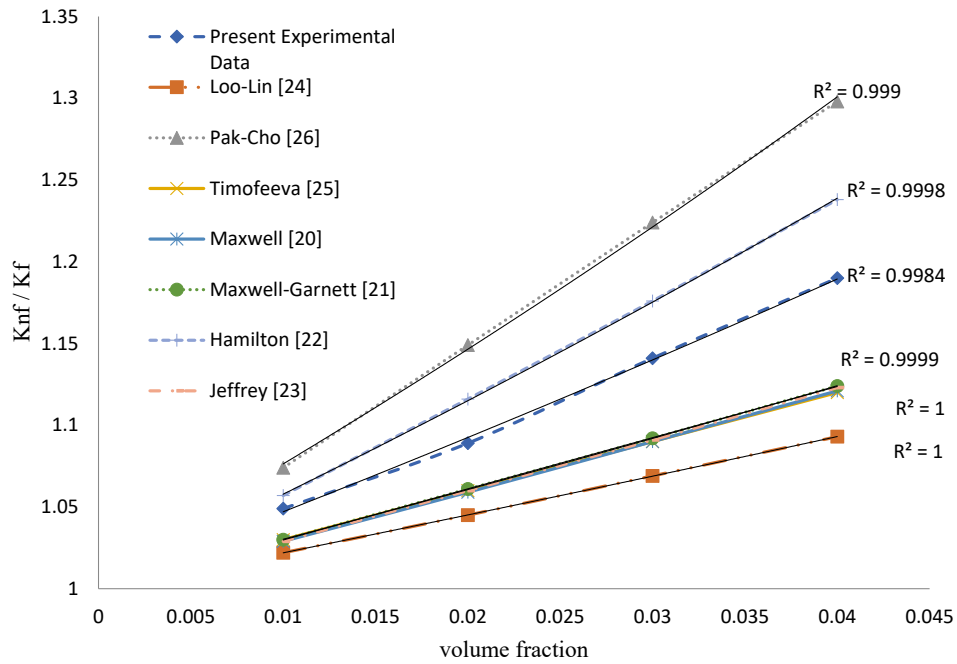


Fig. 9. Display changes in theoretical thermal conductivity coefficient by changing the volume deduction (CuO+Water).

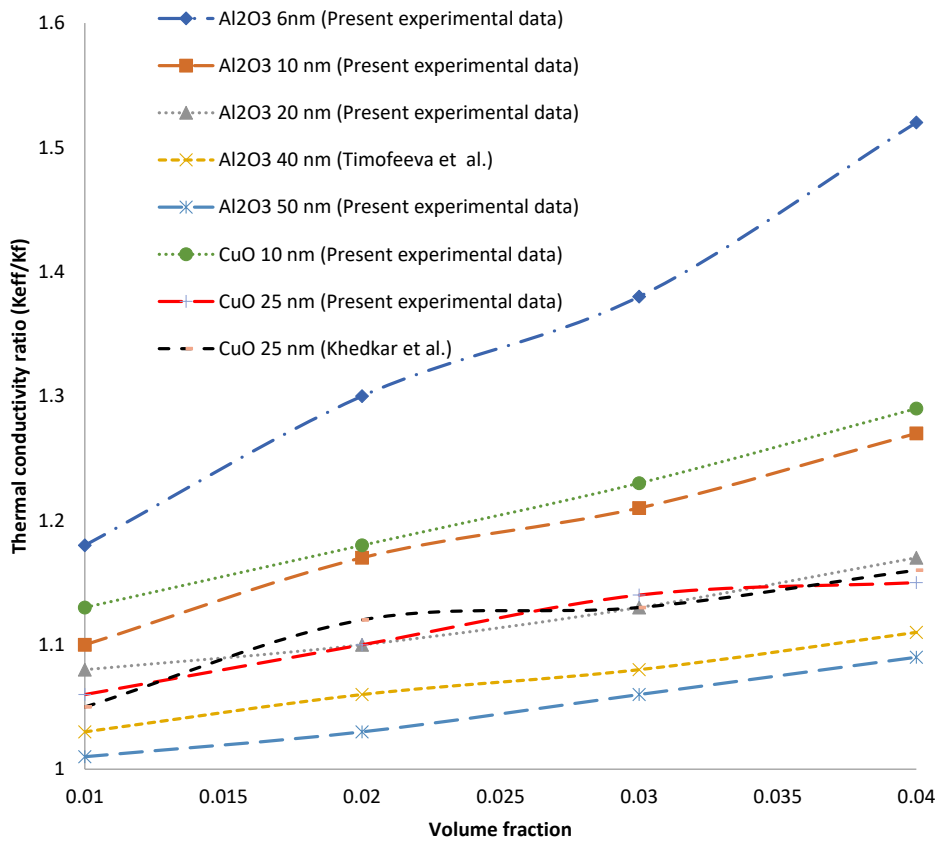


Fig. 10. The effect of nanoparticle size in different volume deduction on the effective thermal conductivity coefficient of CuO+Water and Al₂O₃+Water.

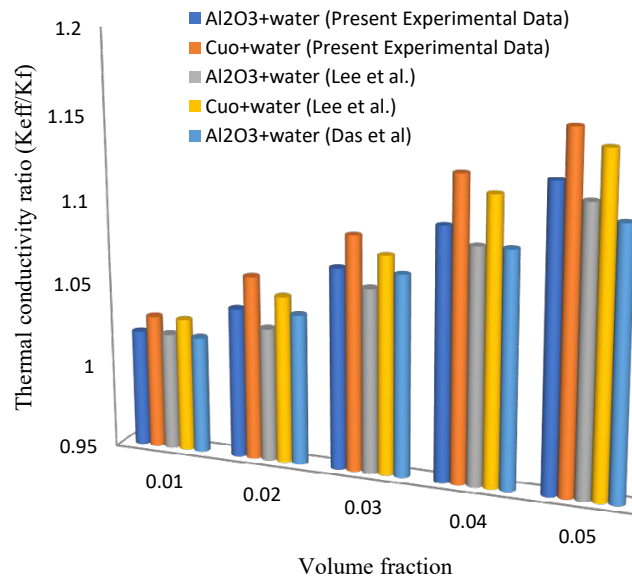


Fig. 11. Investigation of changes in thermal conductivity coefficient of nanofluid Al_2O_3 +Water and CuO+Water with volumetric percentage of nanoparticles.

CuO, the thermal conductivity was improved by 12% when the nanoparticle diameter was reduced from 25 to 10 nm.

Changes in the Nanofluids' Thermal Conductivity with Nanoparticle Volume Fraction

The thermal conductivity of Al_2O_3 -water and CuO-water nanofluids was investigated at different nanoparticle volume fractions (1 to 5 vol%). Fig. 11 illustrates the results of increasing the nanoparticle volume fraction, which can be implemented linearly or nonlinearly. The increase appears differently in different systems with different slopes. The reason is that the thermal conductivity of nanofluids depends on the thermal conductivities of both the base fluid and the nanoparticles. For example, increasing the volume fractions of Al_2O_3 and CuO from 1 to 5% increased the respective nanofluids' thermal conductivity by approximately 10 and 12%. The experimental data were compared with the reports of Lee et al. [59], revealing their consistency.

Measuring the Nanofluid Density

A DA130N density meter was used for the measurements. The results are suggestive of the considerably higher density of nanofluids compared to the water-based fluid. Furthermore, as the nanoparticle volume fraction in the nanofluid

increases, so does the density. Moreover, for the same volume fraction, the CuO-water nanofluid had a higher density than the Al_2O_3 -water (Fig. 12). For example, at 3 vol%, the density of CuO nanofluid was nearly 3% higher than that of the Al_2O_3 nanofluid. Increasing the Al_2O_3 and CuO volume fractions from 1 to 4% in the respective nanofluids increased the density by approximately 7 and 9%. The results were compared with previous studies for validation [50, 60, and 61].

A temperature rise leads to the fluid's expansion, changing its density. It must be noted that different liquids expand at different rates. Accordingly, changes in nanofluid density with temperature were investigated in the following experiment. It was shown that the density decreases with increasing temperature (Fig. 13). However, the decrease depends on the volume fraction of nanoparticles suspended in the nanofluid besides the temperature. For example, at 4 vol%, raising the temperature of the Al_2O_3 -water nanofluid from 20 to 50 °C reduces the density by almost 3%. The results were validated based on data found in the literature [62].

Dynamic Viscosity of the Nanofluids

20 nm nanoparticles were used to measure the viscosity of the Al_2O_3 nanofluid. Temperature is one of the parameters that affect viscosity.

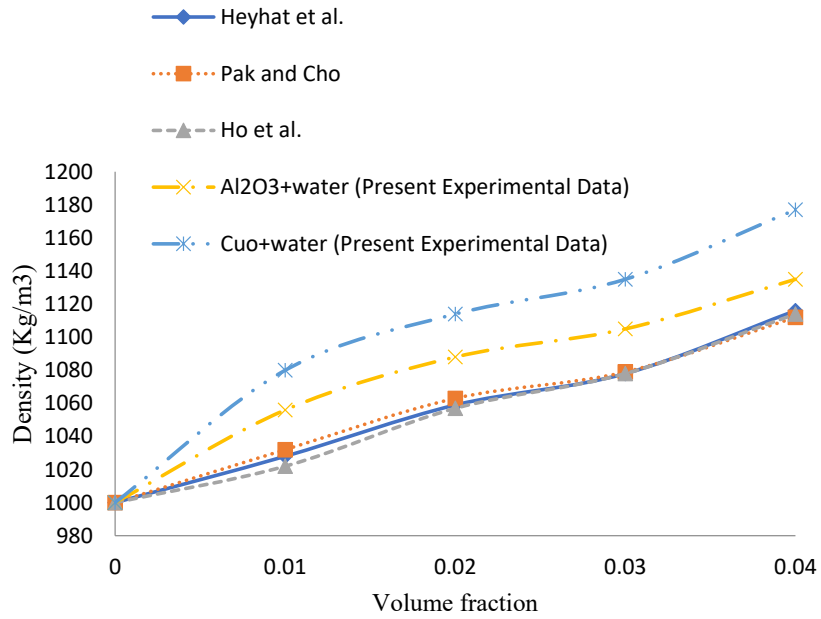


Fig. 12. Nano-fluid density Al_2O_3 +Water and CuO+Water with volumetric percentages 1 to 4.

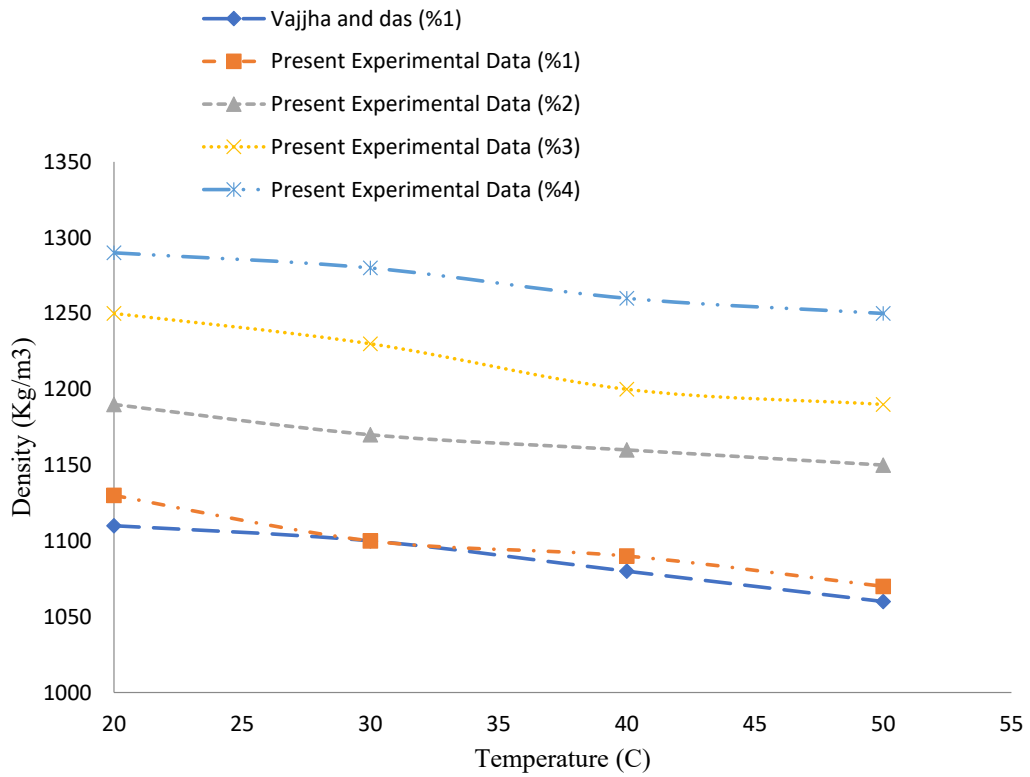


Fig. 13. Nano-fluid Al_2O_3 +Water density changes with temperature changes for 1 to 4 percent volume deduction.

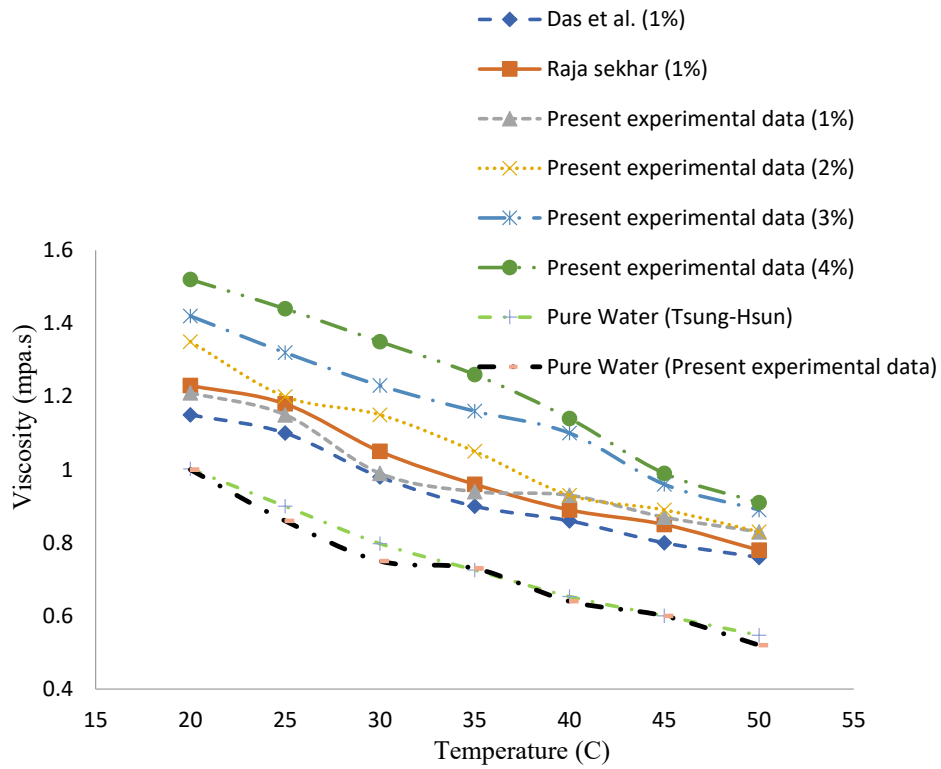


Fig. 14. Viscosity changes of pure water and nanofluid Al₂O₃+Water with temperature changes.

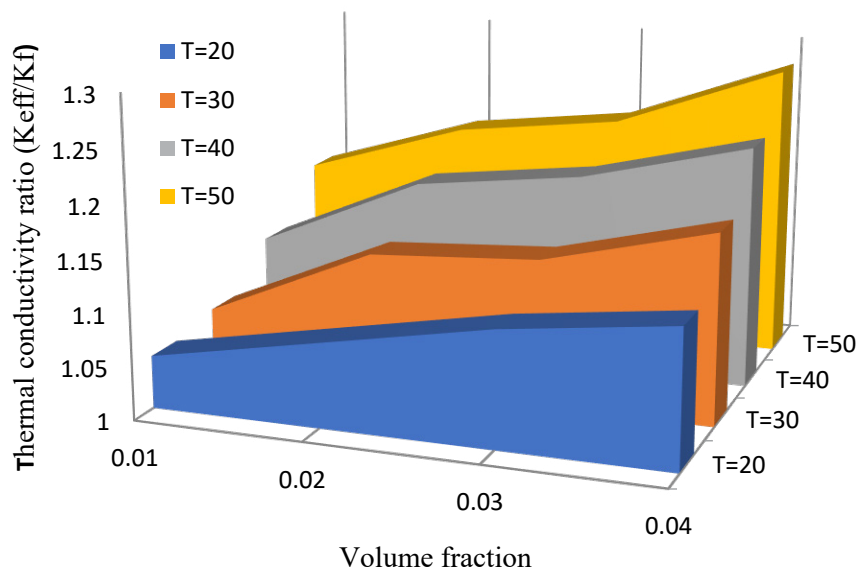


Fig. 15. Changes in the ratio of thermal conductivity coefficient to volume deduction for nanofluid copper oxide in water at different temperatures.

An increase in temperature makes gases more viscous, but the contrary holds for liquids (Fig. 14). This difference can be explained by the effective

factors of viscosity. Results from the literature were used for validation [63, 64].

According to Fig. 14, at 40 °C and 4% volume

fraction, the viscosity increases 78% from the base-fluid level.

Temperature Effects on Nanofluid Thermal Conductivity at Different Volume Fractions

The water-based nanofluid containing 20 nm copper oxide particles was tested at volume fractions of up to 2% in 20 to 50 °C temperature range. Its thermal conductivity was accurately measured and recorded. The test results corresponding to this

nanofluid are shown in Fig. 15.

The accuracy of the results was validated, considering the case with a 1% volume fraction in the 20 and 50 °C temperature range, in comparison with previous reports [65] (Fig. 16).

The experiment was replicated with Al_2O_3 nanofluids with up to 4% nanoparticles (20 nm) in the temperature range between 20 and 50 °C (Fig. 17).

The accuracy of the results was validated,

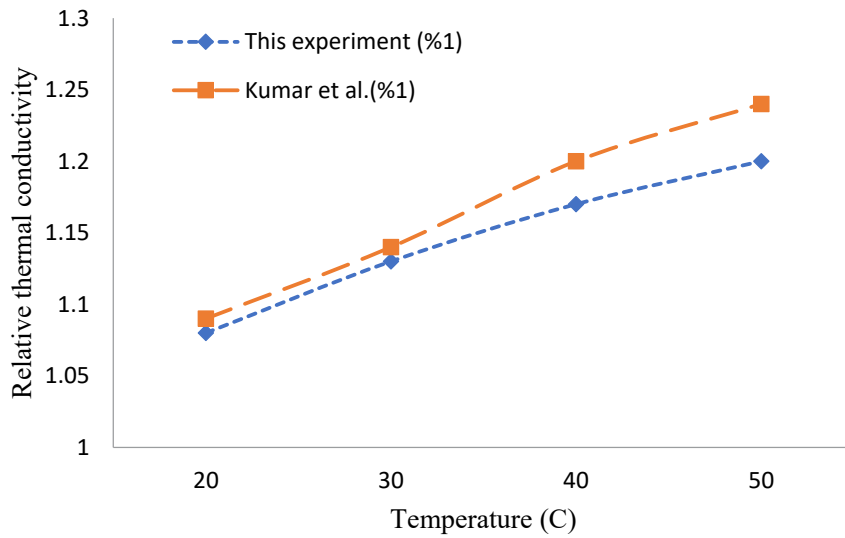


Fig. 16. Comparison of effective thermal conductivity coefficient of copper oxide with a volume of 0.01 at temperatures between 20 and 50 °C with source [64].

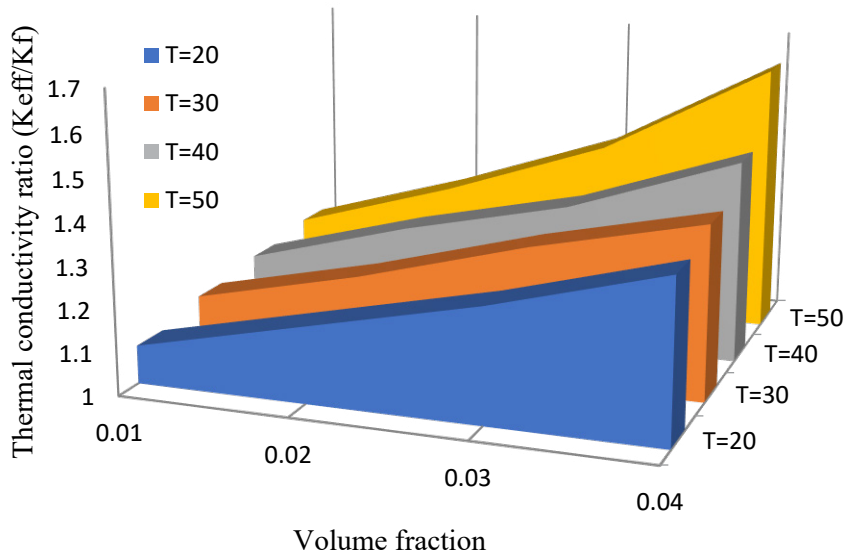


Fig. 17. Changes in the ratio of thermal conductivity coefficient to volume deduction at different temperatures for nanofluid Al_2O_3 + Water.



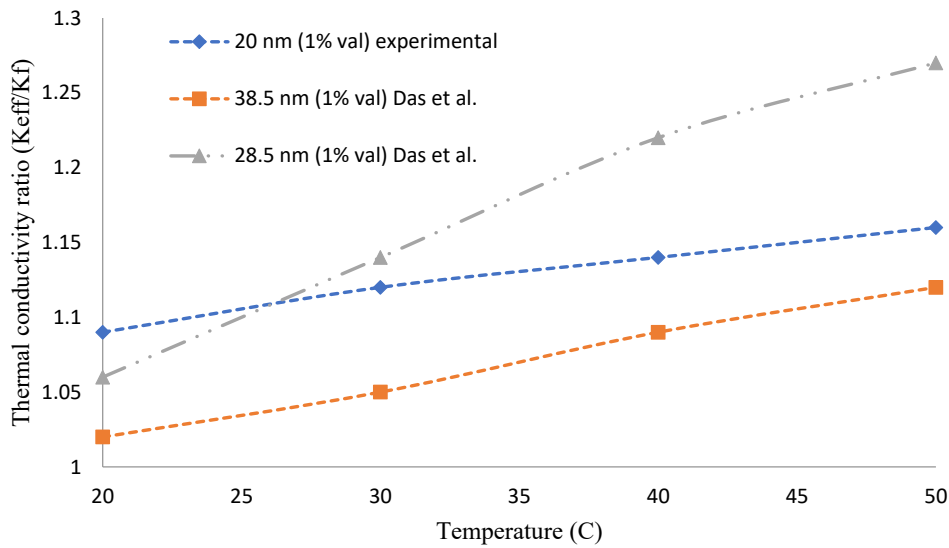


Fig. 18. Comparison of the effective thermal conductivity coefficient of Al_2O_3 with a volume of 0.01 between 20 and 50 °C temperatures.

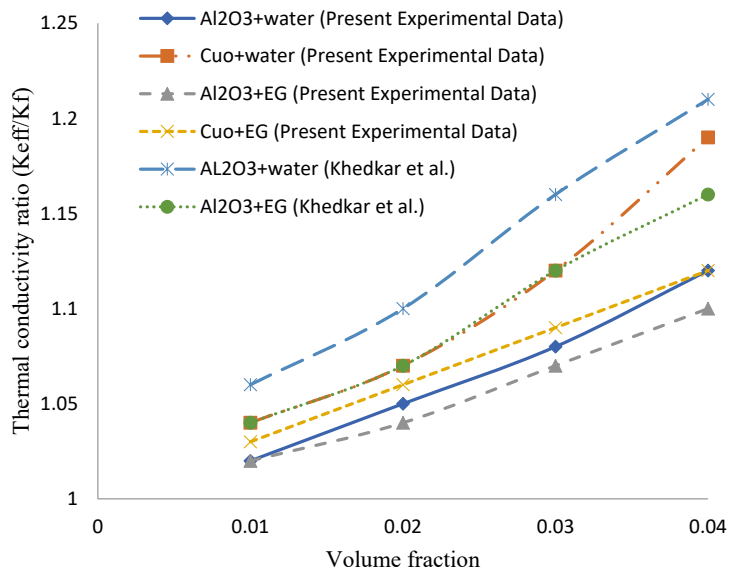


Fig. 19. Comparison of Al_2O_3 and CuO thermal conductivity coefficient with water and ethylene glycol base fluids.

considering the cases with 1 and 4% volume fraction in the 20 and 50 °C temperature range, in comparison with previous reports [65] (Fig. 18).

The results are suggestive of the negligible effects of the temperature on the thermal conductivity coefficient ratio at small volume fractions. However, as the volume fraction increases, the effect of temperature on the thermal conductivity becomes more significant. With the volume fraction increasing, the number of particles suspended in the base fluid increases,

and elevated temperatures promote molecular collision and Brownian motion. For example, in the case of the 1 vol% Al_2O_3 nanofluid, raising the temperature from 20 to 50 °C increases the thermal conductivity by approximately 6%. At 4 vol%, the same temperature increase (20 to 50 °C) improved the thermal conductivity by approximately 18%.

Thermal Conductivity of Water- and EG-Based Al_2O_3 and CuO Nanofluids

The thermal conductivity of the resulting

nanofluids was investigated by mixing different volume fractions of Al_2O_3 and CuO nanoparticles in two common base fluids, namely water and EG. It has been shown that using a base fluid with better thermal properties amplifies the effects of nanoparticles on the nanofluid's thermal conductivity. For example, at 30 °C, the thermal conductivity coefficients of ethylene glycol and water measure 0.28 and 0.62. Considering the case with added CuO, we find that the CuO-EG mix registers a lower thermal conductivity than the mix with water as base fluid (Fig. 19). That is, the thermal conductivity of CuO-water is approximately 3% higher than that of the CuO-EG at 3 vol%.

CONCLUSION

Al_2O_3 and CuO nanoparticles were added to water and EG base fluids at four volume fractions (1-4%) using an electric mixer and magnetic stirring. Nanofluid stability proved to be challenging, and in order for the produced fluids to be applicable, surfactants must be used. Therefore, SDBS and SDS were added to Al_2O_3 and CuO nanofluids, keeping them stable for 22 and 20 days, respectively. The actual thermal conductivity coefficient was obtained by comparing with predicted results. Based on the regression of the experimental results ($R = 0.99$), this value corresponds to the Timofeeva model. Raising the volume fraction and the temperature and reducing the nanoparticle diameter were found to improve the thermal conductivity. Increasing the volume fraction of nanoparticles suspended in the base fluid increases the density. It was also found that increasing the temperature results in a significant drop in viscosity. For example, at 40 °C, adding 4 vol% nanoparticles increased the viscosity by 78% from the base-fluid level. Moreover, at the same volume fraction, the CuO-water had a higher density than Al_2O_3 -water. The better thermal properties of the base fluid are the greater the effects on the nanofluid's thermal conductivity. Since raising the temperature increases the nanofluid's thermal conductivity, it can be concluded that they are the most effective in high-temperature applications.

CONFLICT OF INTEREST

Authors have no conflict of interest.

REFERENCES

- [1] Azari A., Kalbasi M., and Rahimi M., (2014), CFD and experimental investigation on the heat transfer characteristics of alumina nanofluids under the laminar flow regime. *Brazil. J. Chem. Eng.* 31: 469-481.
- [2] Ghadimi A., Saidur R., and Metselaar H., (2011), A review of nanofluid stability properties and characterization in stationary conditions. *Int. J. Heat and Mass Trans.* 54: 4051-4068.
- [3] Abu-Nada E., Masoud Z. N., Oztop H. F., Campo A., (2010), Effect of nanofluid variable properties on natural convection in enclosures. *Int. J. Therm. Sci.* 49: 479-491.
- [4] Murshed S., Leong K. C., Yang C., (2005), Enhanced thermal conductivity of TiO_2 -water based nanofluids. *Int. J. Therm. Sci.* 44: 367-73.
- [5] Das S. K., Choi S. U.S., Yu W., Pradeep T., (2008), Nanofluids: Science and technology. *Nanofluides*. pp. 9.
- [6] Karthik R., Harish Nagarajan R., Raja B., Damodharan P., (2012), Thermal conductivity of CuO-DI Water Nano fluids using 3-x measurement technique in a suspended micro-wire. *Exp. Therm. Fluid Sci.* 40: 1-9.
- [7] Kucharska B., Krawczynska A., Roźniatowski K., Zdunek J., Poplawski K., Sobiecki J. R., (2017), The effect of current types on the microstructure and corrosion properties of Ni/Nano Al_2O_3 composite coatings. *Mater. Technol.* 51: 403-411.
- [8] Ghazvini M., Akhavan-Behdadi M. A., Rasouli E., Raisee M., (2012), Heat transfer properties of nanodiamond-engine Oil nanofluid in laminar flow. *Heat Transf. Eng.* 33: 525-532.
- [9] Leong K. Y., Saidur R., Kazi S. N., (2010), Performance investigation of an automotive car radiator operated with nanofluid-based coolants nanofluid as a coolant in a radiator. *Appl. Therm. Eng.* 30: 2685-2692.
- [10] Leong K. Y., Saidur R., Kazi S. N., Mamun A. H., (2010), Performance investigation of an automotive car radiator operated with nanofluidbased coolants (nanofluid as a coolant in a radiator). *Appl. Therm. Eng.* 30: 2685-2692.
- [11] Syam Sundar L., Sharma K., Naik M., Singh M., (2013), Empirical and theoretical correlations on viscosity of nanofluids :A review. *Renew. Sustain. Energy.* 25: 670-686.
- [12] Pugalenti P., Jayaraman M., Subburam V., (2019), Study of the microstructures and mechanical properties of aluminium hybrid composites with SiC and Al_2O_3 . *Mater. Technol.* 53: 49-55.
- [13] Pastoriza-Gallego M. J., Casanova C., Legido J. L., Pineiro M. M., (2011), CuO in water nanofluid: Influence of particle size and polydispersity on volumetric behaviour and viscosity. *Fluid Phase Equil.* 300: 188-196.
- [14] Singh P., Venkatachalapathy S., Kumaresan G., (2014), Heat transfer studies on condensation using heat pipes. Proceedings of applied mechanics and materials, switzerland: *Trans Tech Publication Inc.* 592: 1617-1621.
- [15] Turkyilmazoglu M., (2015), Analytical solutions of single and multi-phase models for the condensation of nanofluid film flow and heat transfer. *Europ. J. Mech.* 53: 272-277.
- [16] El Mghari H., Louahlia-Gualous H., Lepinasse E., (2015), Numerical study of nanofluid condensation heat transfer in a square microchannel. *Numeric. Heat Transf.* 68: 1242-1265.
- [17] Azimi H., Taheri R., (2015), Electrical conductivity of CuO nanofluids. *Int. J. Nano Dimens.* 6: 77-81.
- [18] Sabbaghi S., Orojloou H., Parvizi M., Saboori R., Sahooli M.,

- (2012), Effect of temperature and time on morphology of CuO nanoparticle during synthesis. *Int. J. Nano Dimens.* 3: 69-73.
- [19] Bhuiyan M. H. U., Saidur R., Mostafizur R. M., Mahbulul I. M., Amalina M. A., (2015), Experimental investigation on surface tension of metal oxide–water nanofluids. *Int. Communic. Heat and Mass Transf.* 65: 82-88.
- [20] Pecora R., (1985), *Dynamic light scattering: Applications of photon correlation spectroscopy.* Springer.
- [21] Chandrasekar M., Suresh S., and Bose A. C., (2010), Experimental investigations and theoretical determination of thermal conductivity and viscosity of Al₂O₃/water nanofluid. *Exp. Termal Fluid Sci.* 34: 210–216.
- [22] Kong L., Sun J., Bao Y., (2017), Preparation, characterization and tribologicalmechanismof nanofluids. *RSC Advances.* 7: 12599–12609.
- [23] Maxwell J. C., (1904), *A Treatise on electricity and magnetism.* second edition. Oxford University Press, Cambridge. p. 435.
- [24] Maxwell Garnett J., (1904), Colours in metal glasses and in metallic films. *Philos. Trans. R. Soc. London.* 203: 385-420.
- [25] Hamilton R. L., Crosser O. K., (1962), Thermal conductivity of heterogeneous tow-component systems. *I & EC Fundam.* 1:182-191.
- [26] Jeffrey D. J., (1973), Conduction through a random suspension of spheres. *Proc. R. Soc. London.* 335: 355-367.
- [27] Lu S., Lin H., (1996), Reflective conductivity of composite containing aligned spherical inclusions of finite conductivity. *J. Appl. Phys.* 79: 6761–6769.
- [28] Timofeeva E. V., Gavrilov A. N., McCloskey J. M., Tolmachev Y. V., (2007), Thermal conductivity and particle agglomeration in alumina nanofluids: experiment and theory. *Phys. Rev.* 76: 061203-061208.
- [29] Pak B. C., Cho Y. I., (1998), Hydraulic and heat transfer study of dispersed fluids with submicron metallic oxide particles. *Exp. Heat Transf.* 11: 151-170.
- [30] Nagasaka Y., Nagashima A., (1981), Absolute measurement of the thermal conductivity of electrically conducting liquids by the transient hot wire method. *J. Phys.* 14: 1435–1440.
- [31] Franco A., (2007), An apparatus for the routine measurement of thermal conductivity of materials for building application based on a transient hot-wire method. *Appl. Therm. Eng.* 27: 2495–2504.
- [32] Wen D., Lin G., Vafaei S., Zhang K., (2009), Review of nanofluids for heat transfer applications. *Particuology.* 7: 141–150.
- [33] Wang X.-Q., Mujumdar A. S., (2008), A review on nanofluids—Part I: Theoretical and numerical investigations. *Braz. J. Chem. Eng.* 25: 613–630.
- [34] Einstein A., (1906), Eineneuebestimmung der moleküldimensionen. *Annals. Phys.* 324: 289–306.
- [35] Krieger I. M., Thomas J. D., (1957), A mechanism for non-newtonian flow in suspensions of rigid spheres. *Transact. Soc. Rheol.* 3: 137–152.
- [36] Nielsen L. E., (1970), Generalized equation for the elastic moduli of composite materials. *J. Appl. Phys.* 41: 4626–4627.
- [37] Mooney M., (1951), The viscosity of a concentrated suspension of spherical particles. *J. Colloid Sci.* 6: 162–170.
- [38] Batchelor G. K., (1977), The effect of Brownian motion on the bulk stress in a suspension of spherical particles. *J. Fluid Mech.* 83: 97–117.
- [39] Lundgren T. S., (1972), Slow flow through stationary random beds and suspensions of spheres. *J. Fluid Mech.* 51: 273–299.
- [40] Brinkman H. C., (1952), The viscosity of concentrated suspensions and solutions. *J. Chem. Phys.* 20: 571-577.
- [41] Chen H., Ding Y., Tan C., (2007), Rheological behaviour of nanofluids. *New J. Phys.* 9: 367-371.
- [42] Frankel N. A., Acrivos A., (1967), On the viscosity of a concentrated suspension of solid spheres. *Chem. Eng. Sci.* 22: 847–853.
- [43] Cheng N. S., Law A. W. K., (2003), Exponential formula for computing effective viscosity. *Powder Technol.* 129: 156–160.
- [44] Kitano T., Kataoka T., Shirota T., (1981), An empirical equation of the relative viscosity of polymer melts filled with various inorganic fillers. *Rheologica. Acta.* 20: 207–209.
- [45] Bicerano J., Douglas J. F., Brune D. A., (1999), Model for the viscosity of particle dispersions. *J. Macromol. Sci.* 39: 561–642.
- [46] Tseng W. J., Chen C. N., (2003), Effect of polymeric dispersant on rheological behavior of nickel–terpineol suspensions. *Mater. Sci. Eng.* 347:145–153.
- [47] Graham A. L., (1981), On the viscosity of suspensions of solid spheres. *Appl. Sci. Res.* 37: 275–286.
- [48] Masoumi N., Sohrabi N., Behzadmehr A., (2009), A new model for calculating the effective viscosity of nanofluids. *J. Phys. D. Appl. Phys.* 42: 055501-055505.
- [49] Pak B. C., Cho Y. I., (1998), Hydraulic and heat transfer study of dispersed fluids with submicron metallic oxide particles. *Exp. Heat Transf.* 11:151-170.
- [50] Kulkarni D. P., Das D. K., Chukwu G. A., (2006), Temperature dependent rheological property of copper oxide nanoparticles suspension (nanofluid). *J. Nanosci. Nanotechnol.* 6: 1150–1154.
- [51] Nguyen C. T., Desgranges F., Roy G., Galanis N., Mare T., Boucher S., Angue Mintsa H., (2007), Temperature and particle-size dependent viscosity data for water-based nanofluids–hysteresis phenomenon. *Int. J. Heat Fluid Flow.* 28:1492–1506.
- [52] Namburu P. K., Das D. K., Tanguturi K. M., Vajjha R. S., (2009), Numerical study of turbulent flow and heat transfer characteristics of nanofluids considering variable properties. *Int. J. Therm. Sci.* 48: 290–302.
- [53] Chandrasekar M., Suresh S., Chandra Bose A., (2010), Experimental investigations and theoretical determination of thermal conductivity and viscosity of Al₂O₃/water nanofluid. *Exp. Therm. Fluid Sci.* 34: 210–216.
- [54] Abu-Nada E., (2009), Effects of variable viscosity and thermal conductivity of Al₂O₃–water nanofluid on heat transfer enhancement in natural convection. *Int. J. Heat Fluid Flow.* 30: 679–690.
- [55] Masoud Hosseini S., Moghadassi A. R., Henneke D. E., (2010), A new dimensionless group model for determining the viscosity of nanofluids. *J. Therm. Anal. Calorim.* 100: 873–877.
- [56] Avsec J., Oblak M., (2007), The calculation of thermal conductivity, viscosity and thermodynamic properties for nanofluids on the basis of statistical nanomechanics. *Int. J. Heat Mass Transf.* 50: 4331–4341.

- [57] Keblinski P., Phillpot S. R., Choi S., Eastman J. A., (2002), Mechanisms of heat flow in suspensions of nano-sized particles (nanofluids). *Int. J. Heat and Mass Transf.* 45: 855-863.
- [58] Lee S., Choi S., Li S., Eastman J. A., (1999), Measuring thermal conductivity of fluids containing oxide nanoparticles. *ASME J. Heat Transf.* 121: 280-289.
- [59] Heyhat M. M., Kowsary F., Rashidi A. M., Alem Varzane Esfehiani S., Amrollahi A., (2012), Experimental investigation of turbulent flow and convective heat transfer characteristics of alumina water nanofluids in fully developed flow regime. *Int. Commun. Heat Mass Transf.* 39: 1272–1278.
- [60] Ho C., Liu W., Chang Y., Lin C., (2010), Natural convection heat transfer of alumina-water nanofluid in vertical square enclosures: an experimental study. *Int. J. Therm. Sci.* 49:1345–1353.
- [61] Vajjha R. S., Das D. K., (2009a), Experimental determination of thermal conductivity of three nanofluids and development of new correlations. *Int. J. Heat Mass Transf.* 52: 4675–4682.
- [62] Das S. K., Putra N., and Roetzel W., (2003a), Pool boiling characteristics of nano-fluids. *Int. J. Heat Mass Transf.* 46: 851–862.
- [63] Raja Sekhar Y., Sharma K. V., (2015), Study of viscosity and specific heat capacity characteristics of water-based Al_2O_3 nanofluids at low particle concentrations. *J. Exp. Nanosc.* 10: 86-102.
- [64] Das S. K., Putra N., Thiesen P., Roetzel W., (2003), Temperature dependence of thermal conductivity enhancement for nanofluids. *J. Heat Transf.* 125: 567-574.